HHS Public Access

Author manuscript

Ann Pancreat Cancer. Author manuscript; available in PMC 2020 December 22.

Published in final edited form as:

Ann Pancreat Cancer. 2020 November ; 3: . doi:10.21037/apc-20-25.

Quantitative metric for assessment of pancreatic ductal adenocarcinoma treatment response in T1-weighted gadolinium-enhanced magnetic resonance imaging

Joy Liau[1], **Srinivasan Vedantham**[2], **Hani M. Babiker**[3], **Travis McGlothin**[4], **Diego R. Martin**[5]

[1]Department of Radiology, University of California at San Diego, San Diego, CA, USA;

[2]Departments of Medical Imaging and Biomedical Engineering, University of Arizona, Tucson, AZ, USA;

[3]Early Phase Clinical Trials Program, University of Arizona Cancer Center, Tucson, AZ, USA;

[4]Department of Medical Imaging, University of Arizona, Tucson, AZ, USA;

[5]Department of Radiology and the Translational Imaging Institute, Houston Methodist Hospital, Houston, TX, USA

Abstract

Background: We theoretically derived a new quantitative metric reflecting the product of T1 signal intensity and contrast media concentration (*T1C*) using first principles for the signal provided by the gradient echo sequence. This metric can be used with conventional gadolinium contrast-enhanced magnetic resonance imaging (CE-MRI) exams. We used this metric to test our hypothesis that gadolinium enhancement changes with pancreatic ductal adenocarcinoma (PDA) treatment response, and that this metric may differentiate responders from non-responders.

Methods: Out of 264 initially identified patients, a final total of 35 patients with PDA were included in a retrospective study of responders (n=24) and non-responders (n=11), which used

Correspondence to: Joy Liau, MD PhD. Department of Radiology, University of California at San Diego, 200 West Arbor Drive #8756, San Diego, CA, 92103-8756, USA. jliau@health.ucsd.edu.

Contributions: (I) Conception and design: J Liau, S Vedantham, HM Babiker, DR Martin; (II) Administrative support: J Liau, S Vedantham; (III) Provision of study materials or patients: J Liau, HM Babiker, DR Martin; (IV) Collection and assembly of data: J Liau, T McGlothlin; (V) Data analysis and interpretation: J Liau, S Vedantham; (VI) Manuscript writing: All authors; (VII) Final approval of manuscript: All authors.

Data Sharing Statement: Available at http://dx.doi.org/10.21037/apc-20-25

Conflicts of Interest: All authors have completed the ICMJE uniform disclosure form (available at http://dx.doi.org/10.21037/apc-20-25). Dr. SV reports grants from NIH/NCI during the conduct of the study. HB serves as an unpaid Section Editor of *Annals of Pancreatic Cancer* from October 2019 to September 2021. The other authors have no conflicts of interest to declare.

Ethical Statement: The authors are accountable for all aspects of the work in ensuring that questions related to the accuracy or integrity of any part of the work are appropriately investigated and resolved. The study was conducted in accordance with the Declaration of Helsinki (as revised in 2013). We obtained prior to initiating research an Institutional Review Board Approval Protocol Number: 1704366654 and further obtained a waiver of personal health information authorization [45 CFR 164.512(i)(2) (ii)] as the use or disclosure of protected health information involves no more than minimal risk to the individuals and the research could not practicably be conducted without the waiver.

changes in cancer antigen 19–9 (CA 19–9) and tumor size as reference standards. *T1C* was computed for the pancreatic mass in the arterial, portal venous, and delayed phases in pre-treatment and post-treatment MRIs. Changes in measurements and correlations with treatment response were assessed by repeated measures analysis of variance and paired *t*-tests.

Results: In the treatment responder group, *T1C* significantly increased in the arterial, portal venous, and delayed phases (P=7.57e–5, P=3.25e–4, P=1.75e–4). In the non-responder group, *T1C* did not significantly change in any phase (P>0.58). Post-treatment *T1C* significantly differed between responders and non-responders (P=0.044) by repeated measures analysis of variance.

Conclusions: *T1C* significantly increases in all phases of CE-MRI in responders to treatment, but does not change in non-responders. *T1C* correlates with treatment response, can be computed from clinical MRI exams, and may be useful as an additional metric to stratify patients undergoing treatment.

Keywords

Pancreatic cancer; treatment response; magnetic resonance imaging (MRI); T1

Introduction

Pancreatic ductal adenocarcinomas (PDAs) are highly lethal cancers for which advances in detection and treatment are greatly needed. Although progress has been made in treatment and outcomes of other major cancers, the lack of early detection and relatively ineffective treatment of PDA, in addition to an apparent increasing incidence, are factors considered in predicting that PDA will be the 2nd leading cause of cancer death in the US by 2030 (1). Medical imaging plays an important role in evaluating PDA treatment response, and continued innovations in imaging are vital for support of trials validating new and improved treatments.

Current methods of assessing treatment response by imaging size measurements and serum tumor biomarkers levels have notable shortcomings in application to pancreatic cancer. Most imaging criteria for evaluating treatment response are based on size [e.g., World Health Organization (WHO) and Response Evaluation Criteria in Solid Tumors (RECIST) Guidelines (2)]. Computed tomography (CT) is the most often used modality to assess PDA, but cannot distinguish tumor margins or residual tumor from fibroinflammatory tissue due to limitations in soft-tissue contrast (3–6), which may adversely impact accuracy of size measurements. When changes in size are equivocal, serum tumor biomarkers can provide a surrogate measure of treatment response. Cancer antigen 19–9 (CA 19–9) is a widely used PDA biomarker, but it can be falsely elevated by benign conditions such as biliary obstruction, pancreatitis, colon cancer, or chronic liver disease, and is not elevated in 5–10% of PDAs (7).

Measurements of longitudinal relaxation time (T1) in magnetic resonance imaging (MRI) have been shown to decrease with treatment response in mouse models of neuroblastoma (8), and fibrosarcoma and melanoma (9), but have not been evaluated for PDA.

An increasing number of studies have assessed pancreatic cancer treatment response with T1-weighted dynamic gadolinium contrast-enhanced magnetic resonance imaging (CE-MRI). CE-MRI studies have shown that antiangiogenic treatment decreases perfusion parameters before detection of a change in tumor size, in a rat model (10) and in human patients (11). Unfortunately, the addition of antiangiogenic therapy to PDA treatment have not shown benefit in clinical trials (12,13) and are no longer commonly utilized. A recent CE-MRI study in human patients treated with currently used regimens (FOLFIRINOX, gemcitabine plus protein-bound paclitaxel, or gemcitabine plus cisplatin) found significantly increased perfusion in PDA tumors responding to therapy. To account for the inherent variability in CE-MRI measurements, an external perfusion phantom was used for calibration (14).

Effective PDA treatment results in therapy-related increased fibrosis and reduced tumor cell volume (15,16). Fibrosis may manifest on CE-MRI as increased contrast uptake on delayed phase T1-weighted images, a property that has been demonstrated in other fibrotic tissues related to cardiac (17) and liver (18) imaging. We hypothesize that treatment-related fibrosis in pancreatic cancer should result in an increased contrast uptake on delayed phase MRI. In patients with tumor response, fibrosis may decrease unenhanced T1 signal intensity (19), while injury response and granulation tissue or remodeled ingrowth of pancreatic acinar tissue may be expected to increase T1 signal intensity (8,9). In the absence of treatment response, we expect little change in the tissue histology or MRI features. To evaluate changes of PDA response to treatment on CE-MRI and to test these hypotheses, we developed a quantitative metric reflecting both T1 signal intensity and contrast uptake that can be computed from standardized clinical MRI exams; we applied this metric in a retrospective study in groups of PDA patients that did, or did not, respond to treatment.

Methods

Patients

The study was conducted in accordance with the Declaration of Helsinki (as revised in 2013). We obtained prior to initiating research an Institutional Review Board Approval Protocol Number: 1704366654 and further obtained a waiver of personal health information authorization [45 CFR 164.512(i)(2) (ii)] as the use or disclosure of protected health information involves no more than minimal risk to the individuals and the research could not practicably be conducted without the waiver.

Patients diagnosed with pancreatic cancer at the University of Arizona Cancer Center from January 2012 to June 2016 were consecutively included. Inclusion criteria were: (I) at least 18 years of age; (II) borderline unresectable, or locally advanced unresectable, or metastatic PDA; (III) MRI examination before and after treatment with chemotherapy and/or radiation; (IV) measurable disease on MRI; and (V) CA 19–9 serum tumor biomarker both expressed and measured at time of MRIs. Patients were included regardless of prior treatment. All patients had fine-needle aspiration or core biopsy tissue sampling by endoscopic ultrasound with histologically confirmed PDA. The stage of cancer was determined by imaging (20).

Further criteria were used to classify two patient groups as (I) responder or (II) non-responder. Patients in the responder group had (I) at least 30% decrease in maximum length after treatment [partial response per RECIST 1.1 (2)] or (II) CA 19–9 decrease by at least 50% with treatment (21,22) without regard to tumor size in cases without metastatic disease. CA 19–9 was not used to assess treatment response in the setting of metastases since the decrease in CA 19–9 may be potentially be due to decrease in metastases rather than the pancreatic mass. The remaining patients comprised the non-responder group. Out of the initially identified 264 patients, these criteria produced a total of 35 patients, with 24 patients in the responder group and 11 patients in the non-responder group (Figure 1, Table 1). Among the 24 responders, 17 were assessed to be responders by size changes, 4 by CA 19–9 changes, and 3 by both size and CA 19–9 changes.

All patients received chemotherapy and/or radiation, with the majority (22/35 patients) receiving FOLFIRINOX (Table 1). All forms of treatment relied on DNA synthesis inhibition (12), unlike prior MRI studies which employed antiangiogenic medications (10,11). Patients received MRIs before and after treatment as part of standard protocol. CA 19–9 was measured at the time of each MRI.

Imaging protocol

All studies were performed on 1.5 or 3.0 T MRI systems (Siemens Medical Solutions, Magnetom Aera/Skyra, Erlangen, Germany). Patients were imaged in the supine position with a phased array torso coil. Patient received 0.05 mmol/kg gadobenate dimeglumine (MultiHance; Bracco Diagnostics, Milan, Italy) intravenous contrast administered by power injection at a rate of 2 mL/s, followed by 20 mL of saline bolus flush at 2 mL/s. Axial three-dimensional T1-weighted gradient echo non-contrast and post-contrast images were acquired through the abdomen at the arterial, venous (45 s) and delayed phases (180 s), each acquired during a breath-hold. Arterial phase images were acquired by automated bolus-triggered technique (Automated Bolus Liver Exam, Liver Lab, Siemens Medical Systems). Technical parameters for the 1.5 T included: TR 4.47 ms, TE 2.2 ms, flip angle 10°, slice thickness 3.0 mm, matrix size 288×216. Technical parameters for the 3.0 T were: TR 3.13 ms, TE 1.13 ms, flip angle 9°, slice thickness 3.0 mm, matrix size 288×216. For both 1.5 and 3 T, technical parameters were: two-dimensional generalized autocalibrating partially parallel acquisitions parallel imaging (2D-GRAPPA) with acceleration factor of 2×2, partial sampling 78% phase field-of-view and 80% phase resolution, and total scanner room utilization times of 25 minutes for abdomen and 45 minutes abdomen and pelvis.

Image analysis

Size measurements and region of interest (ROI) placement—The long axis of the pancreatic masses was measured on the imaging phase where the mass was best visualized (non-contrast or arterial) on axial images (JL with 7 years of abdominal imaging experience). The change of the tumor length with treatment was used to determine partial response with size decrease of at least 30% [RECIST 1.1 guidelines (2)].

Circular ROIs were positioned on the pancreatic mass using the PACS system (Figure 2) to obtain average signal intensities of the pancreatic mass on T1-weighted (I) non-contrast

image (S_0) and post-contrast (II) arterial (S_a), (III) venous (S_v), and (IV) delayed (S_d) phase images. These four measurements were taken for the pre-treatment and post-treatment MRIs of each patient on a single axial slice for each contrast phase. The ROIs were selected to include the majority of the central portion of the pancreatic mass, excluding the sometimes heterogeneous periphery. In large masses that spanned multiple imaging slices, care was taken to select the same portion of the mass in the pre-treatment and post-treatment MRIs. Signal intensity measurements were made by an abdominal imaging fellow (TM with 5 years of abdominal imaging experience), who was blinded to the identity of the pre and post-treatment conditions and whether patients were in the responder or non-responder groups; in order to keep this reader blinded to the efficacy of treatment, he did not make tumor size measurements or view the CA 19–9 data.

Quantitative metric—We sought to develop an objective measure of contrast media uptake in pancreatic masses on conventional pre- and post-contrast T1-weighted images. The contrast media uptake cannot be separated from lesion T1 on conventional MRIs, which lack quantitative T1 mapping. Using first principles for the signal provided by the gradient echo MRI sequence (23), the relationship of T1 to contrast media (24), and our MRI scan parameters, we theoretically derived a quantitative metric ($T1C$) which is the product of longitudinal relaxation time $T1_0$ and contrast media concentration at the post-contrast phase CM_i (Appendix 1):

$$T1C = T1_0 CM_i \quad [1]$$

For each patient, MRI scan, and post-contrast phase, signal-ratio (SR) was computed as:

$$SR_i = \frac{S_i}{S_0} \quad [2]$$

Where S is the signal intensity of the pancreatic mass on the T1-weighted image, 0 is the pre-contrast phase, and i is the post-contrast phase (arterial a, portal venous v, and delayed d). $T1C$ is then calculated by:

$$T1C = \frac{\Delta\, SR_i}{r1(B_0)} = \frac{SR_i^{1/b} - SR_0^{1/b}}{r1(B_0)} \quad [3]$$

Where b is a fit parameter accounting for the two scanner magnetic field strengths used in this study and $r1(B_0)$ is the field-strength dependent relaxivity of the contrast media in plasma (Appendix 1).

Statistical methods—Treatment regimen and biological sex were numerically coded. Since the number of patients treated with capecitabine, HAPa vaccine and radiation therapy were low (2 or 1), they were grouped together. Continuous variables were assessed for normal distribution (Shapiro-Wilk's test) and appropriate summary statistics were obtained. Baseline characteristics of the patient were analyzed to determine if they differed between responders and non-responders. For continuous variables satisfying the normality assumption, independent t-test with Satterthwaite correction was used for analysis. For

variables reported as a proportion, Fisher's exact test was used to determine if they differed between responders and non-responders. For ordinal variables, Wilcoxon-Mann-Whitney test was used for analysis. Generalized linear models (repeated measures analysis of variance) was used to determine if *T1C* at multiple post-contrast phases differed between pre-treatment and post-treatment scans for responders and non-responders. Above analyses were performed using statistical software (SAS®9.4, SAS Institute Inc., Cary, NC, USA). For each patient group and phase, means, standard deviations (SDs), and paired *t*-tests were computed using Matlab (Mathworks, Natick, MA, USA). Effects associated with $P<0.05$ were considered statistically significant.

Results

The baseline characteristics are summarized in Table 1. None of the baseline characteristics significantly differed between responders and non-responders ($P>0.115$). With treatment, the CA 19–9 decreased by 35%±54% in the responder group and increased by 849%±2,339% in the non-responder group. Pancreatic mass size decreased by 35%±15% in the responder group and increased by 10%±37% in the non-responder group.

Repeated measures analysis of variance indicated that the pre-treatment *vs.* post-treatment *T1C* significantly differed between responders and non-responders ($P=0.044$, between-subject effects), with the *T1C* being larger in the post-treatment *vs.* pre-treatment MRI for responders compared to non-responders in all three post-contrast phases. Multivariate tests of within-subject effects analysis showed a significant change in *T1C* between post-contrast phases ($P<0.0001$), that the effect of post-contrast phase on *T1C* was not dependent on whether it was pre-treatment or post-treatment ($P=0.985$), that the effect of post-contrast phase on *T1C* was not dependent on whether the subjects were responders or non-responders ($P=0.247$), and the effect of post-contrast phase on *T1C* was not dependent on the four combinations of pre-/post-treatment and responder/non-responder ($P=0.947$). Figure 3 shows the least-squares means of *T1C* along with the standard error at each post-contrast phase for responders and non-responders.

T1C in responders

Consistent with our hypothesis that pancreatic cancer treatment response can be observed in MRI through altered contrast uptake, we found significant increases in $T1C_a$, $T1C_v$ and $T1C_d$ after treatment ($P=7.57e{-}5$, $3.25e{-}4$ and $2.75e{-}4$, respectively, Figure 3, Table 2). These findings are illustrated in an example subject in the top two rows of Figure 4.

T1C in non-responders

We hypothesized that treatment failure should result in no change in contrast uptake. We found that *T1C* did not change significantly in any of the post-contrast phases in the non-responder group ($P>0.582$, Table 2). The lack of increase in contrast media uptake is illustrated in an example subject in the bottom two rows of Figure 4.

Discussion

We derived a quantitative metric *T1C*, which is linearly related to T1 and contrast media uptake and can be applied to standardized clinical MRI scans. We found that *T1C* was significantly increased after treatment in all post-contrast phases in the responder group but not the non-responder group. In responders, the results imply three possible scenarios could have contributed to the increase in *T1C* in post-treatment MRI: an increase in lesion T1, an increase in contrast uptake between pre-contrast and post-contrast phases, or a combination of the above.

Although the contrast uptake cannot be isolated from lesion T1 in our study, post-contrast images clearly show increased contrast uptake after treatment in the responder group (Figure 4). This is in agreement with recent CE-MRI (14) and perfusion CT (25) studies demonstrating increased blood flow to PDA tumors with successful treatment. These two independent prior reports suggested a similar etiology for the increased perfusion after treatment. They proposed that PDA is normally hypoperfused due to compression of tumor vessels by tumor sclerosis or extracellular matrix scaffold. Effective treatment loosens the scaffold and reduces interstitial pressure, increasing perfusion (14,25). This may correspond to the increased $T1C_a$ and $T1C_v$ in the responder group of our study. Treatment-related inflammation can increase blood flow through angiogenesis and would also produce these results (26,27). Tissue biopsies may be another approach to test these possible correlations.

We found that $T1C_d$ significantly increased with PDA response to treatment, indicating an increase in delayed phase contrast uptake. Histologically, treatment response manifests as the overgrowth and/or replacement of viable tumor with fibrosis (15,16) over time. Fibrosis is associated with an increase in contrast uptake in delayed phase imaging in cardiac (17) and liver (28) MRI, and may be a factor in the $T1C_d$ effect measured in PDA that have responded to treatment.

Decreased T1 can be seen with release of proteins and/or metals from cell and tissue destruction in mouse models of fibrosarcoma and melanoma (9) and with intra-acinar necrosis in colorectal liver metastases (29). The increase in *T1C* we found in our study suggests that positive treatment response produced (I) an increased lesion T1 or (II) an increased contrast uptake to a greater extent than a decreased T1; the latter of these possibilities would be concordant with the cited studies. Also, increased fibrosis has been shown to increase T1 in the heart (19), and the known development of fibrosis with successful treatment response in PDA (15,16) may well have similar signal characteristics. It is possible that PDA responding to treatment may develop various factors that induce change of T1. These changes may be in relation to fibroinflammatory infiltrates that replace tumor, or as a result of cellular apoptosis or necrosis. Future studies, including T1-mapping, may be helpful for further characterization with greater accuracy and sensitivity to T1 properties of PDA, beyond what was possible with standard T1-weighted 3D GRE, as acquired in our study.

Our study has several limitations. Although we started with 264 patients, the final study population was small (n=35) due to the strict inclusion criteria (Figure 1). Patients with

resectable disease did not routinely receive neoadjuvant therapy at our institution, leading to exclusion of 73 patients who went straight to surgery. A further 51 patients elected not to have any treatment. Out of the remaining patients, 78 had incomplete MRIs (missing pre-treatment or post-treatment MRI or insufficient images), 16 had incomplete CA 19–9 measurements, and 11 had masses there were not visible on MRI or were obscured by biliary stents. The retrospective design of this pilot study introduced variability in the timing and type of chemotherapy or radiation and also the MRI timing, relative to treatments. A future prospectively designed study may yield a higher inclusion rate and introduce less opportunities for hidden bias. A larger sample size may produce improved statistical significance. Measures of inter- or intra-observer variability were not performed in this pilot study, and future work including this may be helpful.

We chose tumor size and CA 19–9 changes as the reference standards for treatment response here since they are the most commonly used parameters in clinical practice. Histologic evidence of treatment response was not available in the majority of our patients since they did not undergo surgical resection, and use of progression-free survival or overall survival is complicated by subsequent treatments (i.e., surgical resection, chemotherapy, radiation) received by many patients in our study. Tumor size and CA 19–9 changes are imperfect reference standards and do not always agree, as evidenced by the 21/24 responders here that did not have concordant qualifying tumor size and CA 19–9 changes. An independent marker such as $T1C$ would be especially useful when tumor size and CA 19–9 do not agree, and when tumor size changes are equivocal and CA 19–9 is not measurable. Our preliminary results warrant further testing as a prospective cancer trial which allows for incorporation of additional reference standards.

Several variables affect the $T1C$ values, some of which are present in this study, and others of which would arise with use of different scan protocols. Variations in magnetic field homogeneity are present in every MRI exam. These are included in Eq. [4] in the instrument scaling constant k. Since magnetic field inhomogeneity is relatively constant within a scan session, k is the same in both the numerator and denominator of the ratio in Eq. [7]. This allows it to cancel out and makes $T1C$ relatively insensitive to magnetic field inhomogeneity. Differences in patient weight and physiology may be present in studies of different patients, or in the same patient over time. This could affect the amount of contrast reaching a pancreatic mass, with larger patients or slower circulation resulting in decreased contrast accumulation and decrease in $T1C$. These effects could contribute to variability in the results; however, our results were statistically significant despite the presence of these potential sources of variability. Although not present in our study, use of different scan protocols would also introduce variability if not accounted for. Specifically, b depends on TR and flip angle θ per Eq. [5]. If different parameters from ours were used or the same protocol is not used throughout a study, b will need to be adjusted by performing a power-law fit. Using typical TR values of 2–5 ms (30–32), b ranges from –0.80966 to –6.3308, when flip angle θ is 10°. Typical flip angle θ values of 9°–12° (30–32) produces b-values of –0.6100697 to –0.7342758, when TR is 4.47 ms. Use of a different contrast dose or infusion rate would also introduce variability similar to differences in patient physiology above. For a given contrast media, an increase in contrast dose would increase $T1C$ in a linear manner per Eq. [13]. When different contrast media are used between scans, this is accounted by $r1(B_0)$,

which is the field-strength dependent relaxivity of the contrast media in plasma, as per Eq. [14]. The metric reflects the concentration of the contrast media and hence all factors affecting the concentration of contrast media, such as the infusion speed will also be represented in the metric. Ideally, scan protocols would be uniform within a study population, reducing the sources of error in *T1C* discussed above. Comparison of *T1C* across different studies with different scan protocols are more complex and may require adjustments to the model.

Our *T1C* method may be applied to conventional CE-MRI examinations. Accurate T1-mapping with adequate spatial and temporal resolution would be preferable, providing more accurate and potentially sensitive indicators of intrinsic T1 tumor properties and changes related to treatment, pre- and post-contrast enhancement. However, T1-mapping for this application remains technically challenging, although this may be possible in the future. In addition, we did not find *T1C* values served to prognosticate a responder from a non-responder in the pre-treatment assessment of tumors. Previously, it has been shown that MRI arterial enhancement correlated with PDA grade on histology (33). It may be that we would expect differences in tumor response depending on grade and that we may have found differences in the pre-treatment MRI. This may require a different study design and a larger sample size for delineating possible differences that may prognosticate tumor responsiveness. The data in this study was acquired as part of clinical exams which included diffusion-weighted imaging and apparent diffusion coefficient (ADC) maps. The changes in ADC with treatment were explored but found to be unreliable due to motion artifact. While ADC may be an additional path of investigation, it would require a different methodology for signal acquisition and/or processing.

This preliminary work has potential application and clinical impact for improving assessment of PDA treatment response. PDA has poorly defined margins and is notoriously difficult to measure size accurately and precisely (6). Also, size measurements cannot distinguish between residual tumor and fibroinflammatory tissue after treatment (3–5). A quantitative metric reflecting T1 and contrast uptake would be a useful adjunct to size measurements from imaging. The *T1C* methodology used in our study may be applied to most standard clinical CE-MRIs. Having this additional option is especially important when size changes by imaging are equivocal and CA 19–9 is not available. Given the significant findings in this retrospective study using standard abdominal MRIs, further validation of *T1C* is warranted in larger prospective clinical trials and may be useful in radiomics applications.

Conclusions

We derived a quantitative *T1C* metric that is related to T1 and contrast uptake that can be used with standard clinical CE-MRI. This metric increased in pancreatic cancer responders but not non-responders, possibly providing an alternative to size measurements in assessing treatment response.

Supplementary Material

Refer to Web version on PubMed Central for supplementary material.

Acknowledgments

Funding: This work was supported by 2P30 CA023074 supplement of the Cancer Center Support Grant from the NCI/NIH to the University of Arizona Cancer Center. The contents are solely the responsibility of the authors and do not necessarily reflect the official views of the NIH/NCI.

References

1. Yeo TP. Demographics, epidemiology, and inheritance of pancreatic ductal adenocarcinoma. Semin Oncol 2015;42:8–18. [PubMed: 25726048]
2. Minocha J, Lewandowski RJ. Assessing imaging response to therapy. Radiol Clin North Am 2015;53:1077–88. [PubMed: 26321455]
3. Cassinotto C, Mouries A, Lafourcade JP, et al. Locally advanced pancreatic adenocarcinoma: reassessment of response with CT after neoadjuvant chemotherapy and radiation therapy. Radiology 2014;273:108–16. [PubMed: 24960211]
4. Dudeja V, Greeno EW, Walker SP, et al. Neoadjuvant chemoradiotherapy for locally advanced pancreas cancer rarely leads to radiological evidence of tumour regression. HPB (Oxford) 2013;15:661–7. [PubMed: 23458352]
5. Wagner M, Antunes C, Pietrasz D, et al. CT evaluation after neoadjuvant FOLFIRINOX chemotherapy for borderline and locally advanced pancreatic adenocarcinoma. Eur Radiol 2017;27:3104–16. [PubMed: 27896469]
6. Arvold ND, Niemierko A, Mamon HJ, et al. Pancreatic cancer tumor size on CT scan versus pathologic specimen: implications for radiation treatment planning. Int J Radiat Oncol Biol Phys 2011;80:1383–90. [PubMed: 20708856]
7. Mattes MD, Cardinal JS, Jacobson GM. Delayed radiation-induced inflammation accompanying a marked carbohydrate antigen 19–9 elevation in a patient with resected pancreatic cancer. Radiat Oncol J 2016;34:156–9. [PubMed: 27306770]
8. Jamin Y, Tucker ER, Poon E, et al. Evaluation of clinically translatable MR imaging biomarkers of therapeutic response in the TH-MYCN transgenic mouse model of neuroblastoma. Radiology 2013;266:130–40. [PubMed: 23169794]
9. Weidensteiner C, Allegrini PR, Sticker-Jantscheff M, et al. Tumour T1 changes in vivo are highly predictive of response to chemotherapy and reflect the number of viable tumour cells--a preclinical MR study in mice. BMC Cancer 2014;14:88. [PubMed: 24528602]
10. Raatschen HJ, Fischer S, Zsivcsec B, et al. Non-invasive quantification of anti-angiogenic therapy by contrast-enhanced MRI in experimental pancreatic cancer. Acta Radiol 2014;55:131–9. [PubMed: 23892234]
11. Akisik MF, Sandrasegaran K, Bu G, et al. Pancreatic cancer: utility of dynamic contrast-enhanced MR imaging in assessment of antiangiogenic therapy. Radiology 2010;256:441–9. [PubMed: 20515976]
12. Caparello C, Meijer LL, Garajova I, et al. FOLFIRINOX and translational studies: Towards personalized therapy in pancreatic cancer. World J Gastroenterol 2016;22:6987–7005. [PubMed: 27610011]
13. Saif MW. Pancreatic cancer: Sorafenib: no effect on efficacy of chemotherapy in pancreatic cancer. Nat Rev Gastroenterol Hepatol 2014;11:8–9. [PubMed: 24322903]
14. Kim H, Morgan DE, Schexnailder P, et al. Accurate therapeutic response assessment of pancreatic ductal adenocarcinoma using quantitative dynamic contrast-enhanced magnetic resonance imaging with a point-of-care perfusion phantom: a pilot study. Invest Radiol 2019;54:16–22. [PubMed: 30138218]
15. Hartman DJ, Krasinskas AM. Assessing treatment effect in pancreatic cancer. Arch Pathol Lab Med 2012;136:100–9. [PubMed: 22208494]

16. Pai RK, Pai RK. Pathologic assessment of gastrointestinal tract and pancreatic carcinoma after neoadjuvant therapy. Mod Pathol 2018;31:4–23. [PubMed: 28776577]
17. Vogel-Claussen J, Rochitte CE, Wu KC, et al. Delayed enhancement MR imaging: utility in myocardial assessment. Radiographics 2006;26:795–810. [PubMed: 16702455]
18. Martin DR, Lauenstein T, Kalb B, et al. Liver MRI and histological correlates in chronic liver disease on multiphase gadolinium-enhanced 3D gradient echo imaging. J Magn Reson Imaging 2012;36:422–9. [PubMed: 22566123]
19. Okur A, Kantarci M, Kizrak Y, et al. Quantitative evaluation of ischemic myocardial scar tissue by unenhanced T1 mapping using 3.0 Tesla MR scanner. Diagn Interv Radiol 2014;20:407–13. [PubMed: 25010366]
20. Tamm EP, Silverman PM, Charnsangavej C, et al. Diagnosis, staging, and surveillance of pancreatic cancer. AJR Am J Roentgenol 2003;180:1311–23. [PubMed: 12704043]
21. Ishii H, Okada S, Sato T, et al. CA 19–9 in evaluating the response to chemotherapy in advanced pancreatic cancer. Hepatogastroenterology 1997;44:279–83. [PubMed: 9058159]
22. Ko AH, Hwang J, Venook AP, et al. Serum CA19–9 response as a surrogate for clinical outcome in patients receiving fixed-dose rate gemcitabine for advanced pancreatic cancer. Br J Cancer 2005;93:195–9. [PubMed: 15999098]
23. Bernstein MA, King KF, Zhou XJ. Handbook of MRI Pulse Sequences. Burlington: Elsevier Inc; 2004.
24. Rohrer M, Bauer H, Mintorovitch J, et al. Comparison of magnetic properties of MRI contrast media solutions at different magnetic field strengths. Invest Radiol 2005;40:715–24. [PubMed: 16230904]
25. Hamdy A, Ichikawa Y, Toyomasu Y, et al. Perfusion CT to assess response to neoadjuvant chemotherapy and radiation therapy in pancreatic ductal adenocarcinoma: initial experience. Radiology 2019;292:628–35. [PubMed: 31287389]
26. Costa C, Incio J, Soares R. Angiogenesis and chronic inflammation: cause or consequence? Angiogenesis 2007;10:149–66. [PubMed: 17457680]
27. Libby P Inflammatory mechanisms: the molecular basis of inflammation and disease. Nutr Rev 2007;65:S140–6. [PubMed: 18240538]
28. Petitclerc L, Sebastiani G, Gilbert G, et al. Liver fibrosis: review of current imaging and MRI quantification techniques. J Magn Reson Imaging 2017;45:1276–95. [PubMed: 27981751]
29. Milot L, Guindi M, Gallinger S, et al. MR imaging correlates of intratumoral tissue types within colorectal liver metastases: a high-spatial-resolution fresh ex vivo radiologic-pathologic correlation study. Radiology 2010;254:747–54. [PubMed: 20123902]
30. Li XH, Zhu J, Zhang XM, et al. Abdominal MRI at 3.0 T: LAVA-Flex compared with conventional fat suppression T1-weighted images. J Magn Reson Imaging 2014;40:58–66. [PubMed: 24222639]
31. Donato H, França M, Candelária I, et al. Liver MRI: from basic protocol to advanced techniques. Eur J Radiol 2017;93:30–9. [PubMed: 28668428]
32. Chang KJ, Kamel IR, Macura KJ, et al. 3.0-T MR imaging of the abdomen: comparison with 1.5 T. Radiographics 2008;28:1983–98. [PubMed: 19001653]
33. Lauenstein TC, Martin DR, Sarmiento JM, et al. Pancreatic adenocarcinoma tumor grade determination using contrast-enhanced magnetic resonance imaging. Pancreas 2010;39:71–5. [PubMed: 19745775]

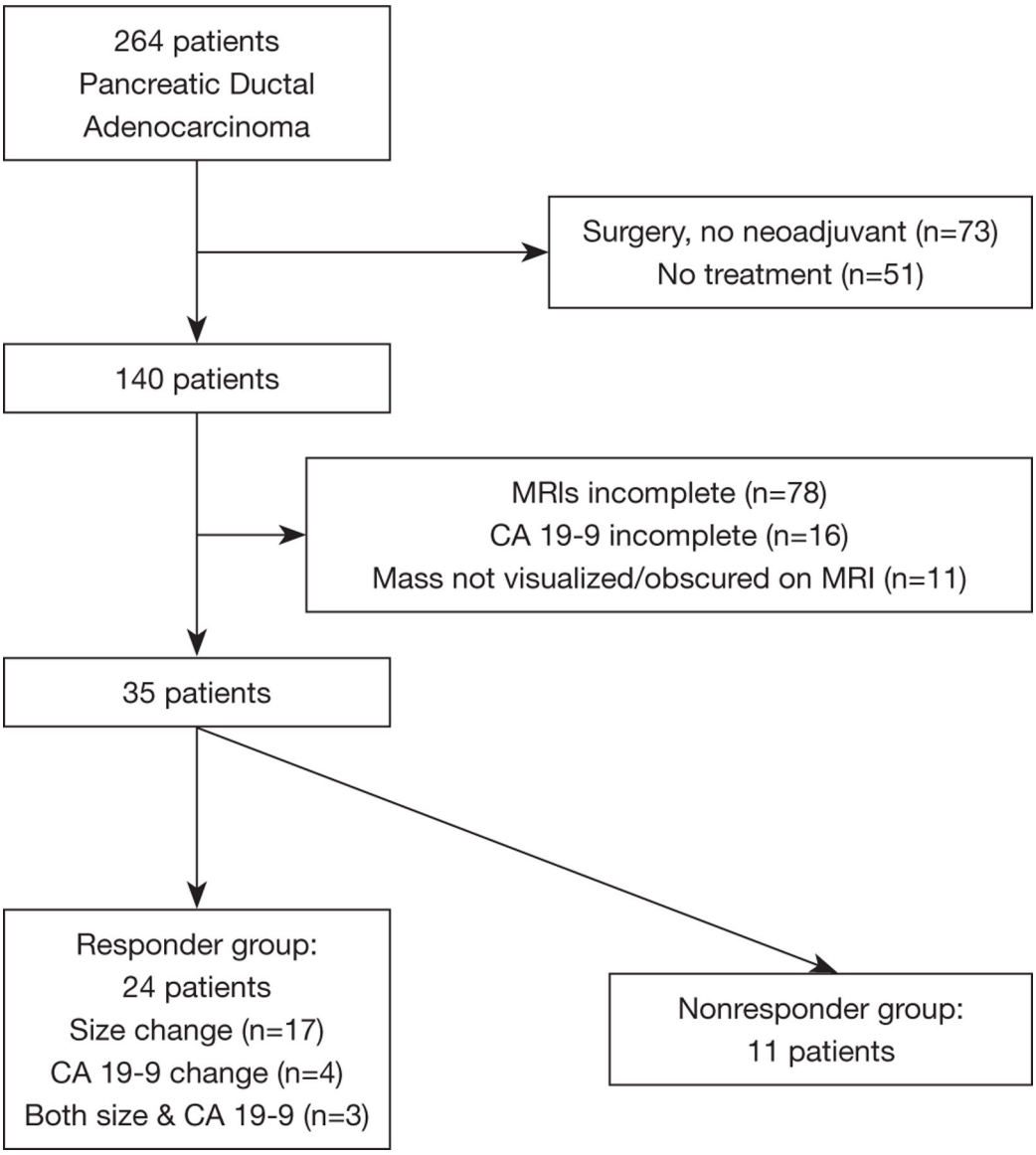

Figure 1.
Patient inclusion and exclusion criteria. MRI, magnetic resonance imaging; CA 19–9, cancer antigen 19–9.

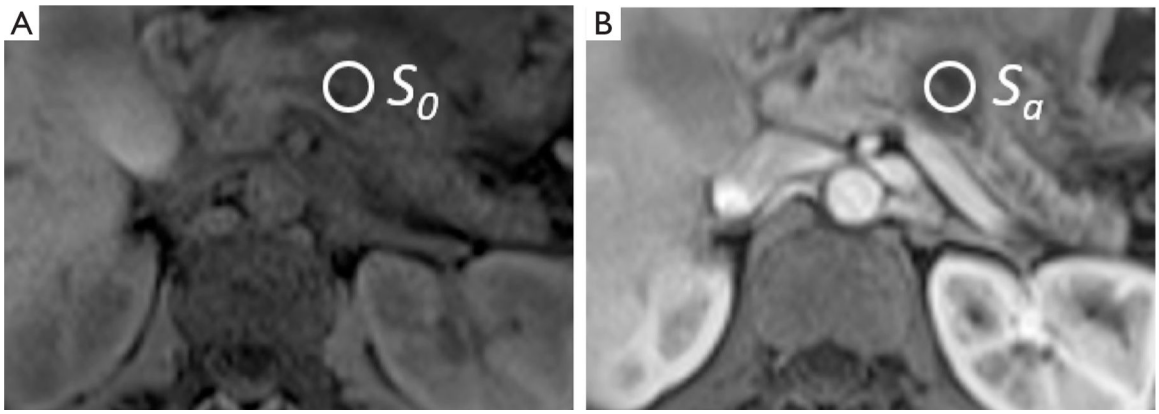

Figure 2.

Example ROIs for patient 1. ROIs (white circles) of the pancreatic mass on T1-weighted axial (A) non-contrast image of the abdomen (S_0) and (B) arterial phase image of the abdomen (S_a). ROIs, regions of interest.

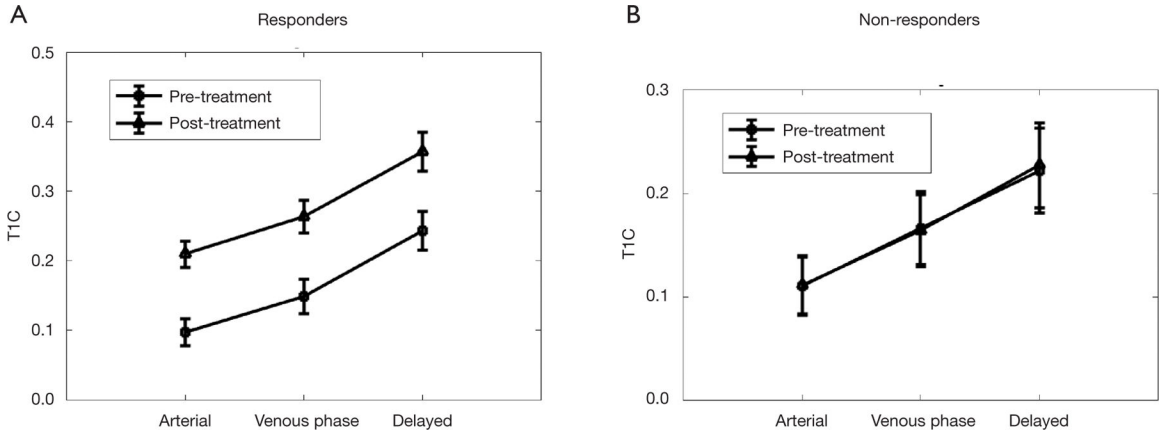

Figure 3.

The least-squares means of the quantitative metric *T1C* along with the standard error at each post-contrast phase for (A) responders and (B) non-responders. There is a significant increase in *T1C* in post-treatment MRI in responders compared to non-responders (P=0.044), and this increase was not dependent on post-contrast phase (P=0.947). MRI, magnetic resonance imaging.

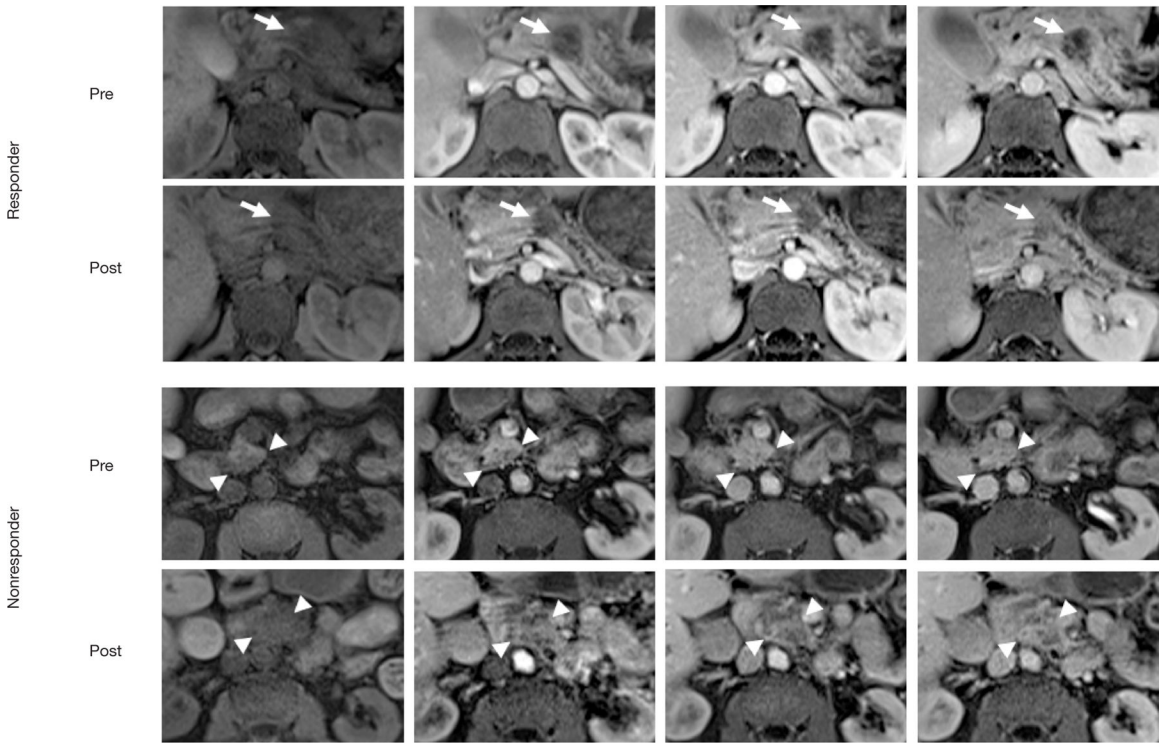

Figure 4.

Treatment response examples. Example T1-weighted axial images of the abdomen without intravenous contrast (first column) and in the arterial (second column), venous (third column), and delayed (fourth column) phases. Subject 1 from the responder group before (first row, size =2.7 cm, CA 19–9 =374 U/mL) and after (second row, size =1.7 cm, CA 19–9 =406 U/mL) treatment showed increase in contrast uptake by the pancreatic body mass (white arrow) with successful treatment. Subject 2 from the non-responder group before (third row, size =1.9 cm, CA 19–9 =39 U/mL) and after (fourth row, size =3.6 cm, CA 19–9 =3,003 U/mL) treatment showed decrease contrast uptake in the pancreatic head mass (white arrowheads). CA 19–9, cancer antigen 19–9.

Table 1

Baseline characteristics

Characteristics	Non-responder (n=11)	Responder (n=24)	P value
Age (years)	68.9±8.2	65.1±10.6	0.257
No. of females	5/11 (45.5%)	11/24 (45.8%)	1.000
Size (cm)	3.17±1.27	3.49±0.91	0.471
CA 19–9 (U/mL)	2,901.9±5,862.1	2,898.6±5,612.1	1.000
Treatment regimen			0.115
Gemcitabine ± protein-bound paclitaxel	2/11 (18.2%)	6/24 (25.0%)	
FOLFIRINOX ± pegph20	7/11 (63.6%)	15/24 (62.5%)	
Other[§]	2/11 (18.2%)	3/24 (12.5%)	
Pre-treatment MRI (days before start of treatment)[†]	22 [7–38]	22 [10.5–31.5]	0.422
Post-treatment MRI (days after start of treatment)[†]	85 [53–105]	75.5 [52.5–82.5]	0.147
Disease stage			
Borderline	6/11 (54.5%)	11/24 (45.8%)	
Locally advanced	–	3/24 (12.5%)	
Metastatic	5/11 (45.5%)	10/24 (41.7%)	
Borderline tumors resected	3/6 (50.0%)	7/11 (63.6%)	

[†], Reported as median [inter-quartile range].

[§], Other treatment regimens include HAPa vaccine (1 responder), capecitabine (1 each of responder and non-responder), and radiation therapy (1 each of responder and non-responder). CA 19–9, cancer antigen 19–9; MRI, magnetic resonance imaging.

Table 2

Simple means and SDs for the quantitative metric

Patient group	Quantitative metric	Pre-treatment (mean ± SD)	Post-treatment (mean ± SD)
Responder	$T1C_a$	0.10±0.09	0.21±0.10
	$T1C_v$	0.15±0.11	0.26±0.12
	$T1C_d$	0.24±0.13	0.36±0.15
Non-responder	$T1C_a$	0.10±0.09	0.10±0.06
	$T1C_v$	0.17±0.14	0.14±0.07
	$T1C_d$	0.22±0.13	0.21±0.13

SD, standard deviation.